

## Surface termination effects on oxygen reduction reaction rate at fuel cell cathodes

Yuri A. Mastrikov<sup>1,3</sup>, Rotraut Merkle<sup>2</sup>, Eugene A. Kotomin<sup>1,2</sup>, Maija M. Kuklja<sup>3</sup>, Joachim Maier<sup>2</sup>

<sup>1</sup> Institute of Solid State Physics, University of Latvia, Riga, Latvia

<sup>2</sup> Max Planck Institute for Solid State Research, Stuttgart, Germany

<sup>3</sup> Materials Science and Engineering Department, University of Maryland, College Park, Maryland, USA

### Supplementary Information

**Table A1.** US-PAW potentials for core electrons

Element	Potential type	Valence electrons	Energy cut-off, eV
La	standard	$5s^2 6s^2 5p^6 5d^1$	219.313
Sr	<i>s</i> semi core	$4s^2 4p^6 5s^2$	229.282
Mn	<i>p</i> semi core	$3p^6 4s^1 3d^6$	269.865
O	standard	$2s^2 2p^4$	400.000

**Table A2:** Ion and layer charges (in *e* per formula unit) for LSM slabs without  $V_O^{\bullet\bullet}$  (data taken from ref. <sup>[1]</sup>). The charges in the central layer of the slabs are close to the bulk values with the same average Mn oxidation state, cf. Fig. 2. Based on the charges of surface O ions that are within  $\pm 0.09 e$  of the bulk charges, the O ions in the surface layers can also be assigned to oxide ions "O<sup>2-</sup>".

$x_{Sr}=0$	LaO termination av. Mn <sup>2.67+</sup>				$x_{Sr}=0.5$	(La,Sr)O termination av. Mn <sup>3.25+</sup>			
	La	Mn	O	plane	La	Sr	Mn	O	plane
surf	1.99		-1.34	0.64	2.00	1.57		-1.33	0.45
		1.59	-1.29	-0.99			1.78	-1.24	-0.70
	2.07		-1.30	0.77	2.09	1.58		-1.24	0.60
central		1.69	-1.27	-0.85			1.78	-1.24	-0.70
$x_{Sr}=0$	MnO <sub>2</sub> termination av. Mn <sup>3.33+</sup>				$x_{Sr}=0.5$	MnO <sub>2</sub> termination av. Mn <sup>3.63+</sup>			
	La	Mn	O	plane	La	Sr	Mn	O	plane
surf		1.69	-1.20	-0.71			1.77	-1.14	-0.51
	2.09		-1.20	0.89	2.09	1.59		-1.18	0.66
		1.83	-1.21	-0.59			1.88	-1.16	-0.44
central	2.08		-1.25	0.83	2.09	1.57		-1.25	0.58

**Table A3:** Bulk oxygen vacancy formation energies  $E_{V_O}$  in eV (relative to gaseous  $\frac{1}{2} O_2$ ) for the first and second  $V_O^{\bullet\bullet}$  created in the  $2 \times 2 \times 2$  LSM supercell. The initial average Mn oxidation state (before  $V_O^{\bullet\bullet}$  further formation) is indicated. For LSM25 and LSM50 the values are averaged over configurations with different local coordination of the  $V_O^{\bullet\bullet}$  by Sr; this leads to variations in the energy around the given average by  $\pm 0.09$  eV and  $\pm 0.04$  eV, respectively. The fact that for the same 3+ oxidation state the formation of the second  $V_O^{\bullet\bullet}$  in LS25M is easier by  $\sim 0.2$  eV than for the first  $V_O^{\bullet\bullet}$  in LM indicates an additional effect by the variation of the Sr content (similar for LS25M and LS50M in 3.25+ oxidation state).

LM 2.75+	LM 3.00+	LS25M 3.00+	LS25M 3.25+	LS50M 3.25+	LS50M 3.50+
4.62	4.66	4.48	4.58	4.29	3.25
second $V_O^{\bullet\bullet}$	first $V_O^{\bullet\bullet}$	second $V_O^{\bullet\bullet}$	first $V_O^{\bullet\bullet}$	second $V_O^{\bullet\bullet}$	first $V_O^{\bullet\bullet}$

**Table A4:** Surface oxygen vacancy formation energies  $E_{V_O^{\bullet}}$  in eV (relative to gaseous  $\frac{1}{2} O_2$ ) for symmetrical 7-layer LSM slabs with (001) (La,Sr)O and  $MnO_2$  termination. The rhombohedral symmetry leads to several different configurations for each termination. There are 4 symmetry-inequivalent positions in each surface layer.

LM LaO	LS25M (La,Sr)O	LS50M (La,Sr)O	LM $MnO_2$	LS25M $MnO_2$	LS50M $MnO_2$
4.97	4.84	4.34	3.74	2.99	1.94
4.99	4.86	4.35	3.74	3.02	1.95
5.19	4.95	4.35	3.75	3.11	1.95
*	4.96	4.35	4.04	3.17	1.97

\* no data available, the slab had reconstructed

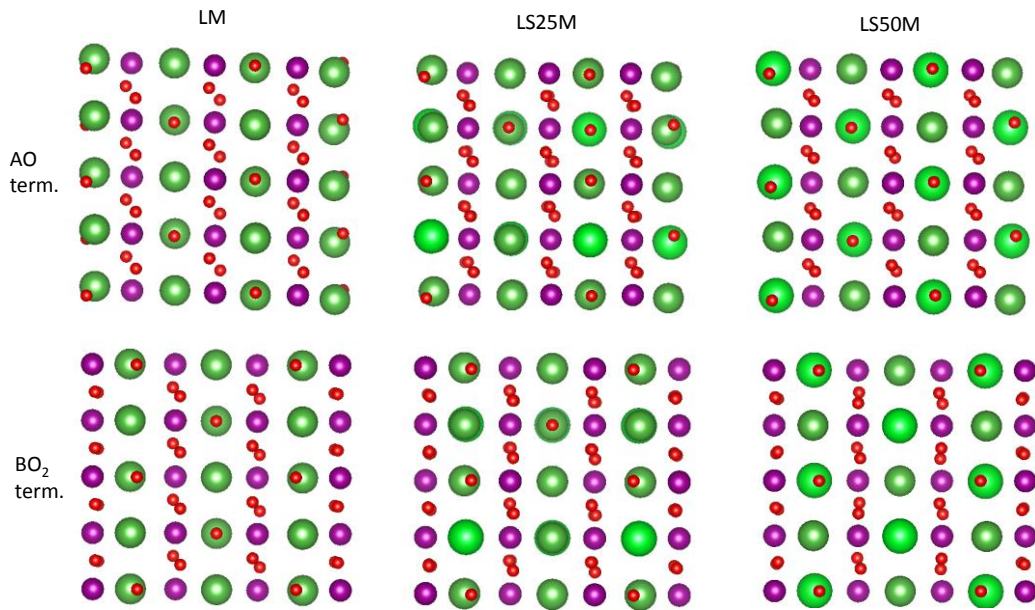


**Figure A1:** Side view of LM, LS25M and LS50M slabs, illustrating the different splitting into sub-planes for AO and  $BO_2$  terminations (Sr = larger green spheres). The splitting into sub-planes contributes to the compensation of the surface dipoles; for AO termination the O are displaced by  $\approx 0.4 \text{ \AA}$  outwards, for the  $MnO_2$  termination the two O per Mn are displaced by  $\approx 0.2 \text{ \AA}$  inwards. However, owing to the larger Bader charges of La as well as oxygen ions in the AO surface layer compared to Mn, O for the  $BO_2$  termination (Table A1), the contribution of the surface rumpling to compensate the surface dipole is larger for AO although in the  $MnO_2$  layer 2 O per formula unit are displaced.

**Table A5:** Charges, distances and energies (relative to gaseous  $\frac{1}{2}$  O<sub>2</sub> for atomic adsorbates, to O<sub>2</sub> for molecular adsorbates) of adsorbed oxygen species on "hollow" sites of 7-plane (001) (La,Sr)O and atop Mn for (001) MnO<sub>2</sub> LSM terminations. For tilted molecular species (cf. Fig. 5b), O\*<sub>ad</sub> indicates the atom close to the surface, surface layer oxide ions are denoted by O<sub>surf</sub>. The octahedral tilting pattern of the LSM slab and different positions relative to Sr surface atoms give rise to several configurations.

species	adsorption energ./eV	charge/ <i>e</i>		O-O dist. /Å	distance /Å to		distance /Å to	
		O* <sub>ad</sub>	O <sub>ad</sub>		La	La' or Sr	O <sub>surf</sub>	O' <sub>surf</sub>
O	-4.31	-1.24		n/a	2.14	2.19	2.89	2.92
O	-4.35	-1.19		n/a	2.15	2.20	2.89	3.03
O <sub>2</sub> tilted	-4.87	-0.72	-0.59	1.46	2.25	2.25	3.08/3.09	3.47/3.57
O <sub>2</sub> horiz.	-5.59	-0.69	-0.71	1.49	2.39/2.48	2.37/2.51	2.72	2.77
LS25M (La,Sr)O								
O	-2.90	-1.27		n/a	2.01	2.38Sr	2.91	2.93
O	-3.00	-1.23		n/a	2.22	2.12	2.79	2.80
O	-3.11	-1.28		n/a	2.03	2.38Sr	2.91	2.95
O	-3.13	-1.27		n/a	2.02	2.39Sr	2.88	2.96
O	-3.22	-1.28		n/a	2.03	2.37Sr	2.98	3.00
O	-3.32	-1.24		n/a	2.17	2.18	2.82	2.82
O	-3.40	-1.24		n/a	2.16	2.19	2.80	2.84
O	-3.45	-1.24		n/a	2.17	2.18	2.81	2.84
O <sub>2</sub> tilted	-3.45	-0.62	-0.74	1.47	2.21	2.30Sr	3.36/3.40	2.96/2.98
O <sub>2</sub> tilted	-3.52	-0.59	-0.72	1.43	2.19	2.39Sr	2.97/3.13	3.34/3.75
O <sub>2</sub> tilted	-3.70	-0.64	-0.74	1.48	2.21	2.31Sr	3.28/3.86	2.91/3.02
O <sub>2</sub> tilted	-3.74	-0.63	-0.74	1.47	2.19	2.30Sr	3.47/3.60	2.93/3.03
O <sub>2</sub> tilted	-3.85	-0.71	-0.61	1.46	2.22	2.25	2.90/2.92	3.33/3.42
O <sub>2</sub> tilted	-3.91	-0.71	-0.61	1.46	2.22	2.25	2.89/2.93	3.30/3.48
O <sub>2</sub> tilted	-3.95	-0.71	-0.61	1.46	2.24	2.26	2.88/2.91	3.31/3.39
O <sub>2</sub> horiz.	-4.03	-0.70	-0.70	1.49	2.31/2.64	2.36/2.47	2.70	2.79
LS50M (La,Sr)O								
O	-1.58	-1.25		n/a	1.99	2.44Sr	2.88	2.89
O	-1.68	-1.26		n/a	2.01	2.45Sr	2.83	2.88
O	-1.84	-1.26		n/a	2.02	2.44Sr	2.85	2.92
O	-1.86	-1.27		n/a	2.02	2.45Sr	2.92	2.94
O <sub>2</sub> tilted	-2.34	-0.65	-0.55	1.37	2.33	2.51Sr	2.86/2.95	3.37/3.47
O <sub>2</sub> tilted	-2.39	-0.56	-0.47	1.37	2.34	2.52Sr	2.84/2.93	3.43/3.45
O <sub>2</sub> tilted	-2.46	-0.60	-0.49	1.40	2.36	2.45Sr	2.85/2.94	3.42/3.58
O <sub>2</sub> tilted	-2.47	-0.58	-0.47	1.38	2.32	2.51Sr	2.95/3.00	3.37/3.48
O <sub>2</sub> horiz.	-1.96	-0.44	-0.42	1.36	2.50Sr	2.52Sr	2.86	2.86
O <sub>2</sub> horiz.	-2.00	-0.63	-0.67	1.47	2.28	2.30	2.86	2.90

For atomic and molecular oxygen species on LS25M, the adsorption energies tend to be about 0.2 eV more negative when the species is absorbed between two La instead of one La and one Sr. The bond length to Sr is larger than to La, in line with the larger ionic radius of Sr<sup>2+</sup>. The charge of adsorbed atomic O species on (La,Sr)O termination is comparable to that of bulk oxide ions (-1.24 to -1.27 *e*,

table A1), thus the species can be assigned to doubly charged adsorbates  $O_{ad}^{2-}$ . For LS25M the charge is systematically more negative by 0.04  $e$  when adsorbed close to Sr. Molecular adsorbates with O-O distance  $\leq 1.4$  Å on LS50M can be assigned to superoxide ( $O_2^-$ ), while longer O-O bonds on LM, LS25M correspond to peroxide ( $O_2^{2-}$ , larger occupation of antibonding orbitals), cf. Fig. A2. The adsorbed superoxide species have significantly longer average distances to the surface La/Sr ions ( $\approx 2.4$  Å) than the peroxide species ( $\approx 2.25$  Å).

species	adsorption energy / eV	charge / $e$ $O_{ad}^*$ $O_{ad}$	O-O dist. / Å	distance / Å to Mn
LM MnO <sub>2</sub>				
O	-1.07	-0.69	n/a	1.62
O	-1.17	-0.55	n/a	1.62
O <sub>2</sub> tilted	-1.43	-0.31 -0.10	1.28	1.93/2.83
O <sub>2</sub> tilted	-1.45	-0.28 -0.12	1.27	1.92/2.82
LS25M MnO <sub>2</sub>				
O	-1.08	-0.57	n/a	1.59
O	-1.09	-0.58	n/a	1.60
O <sub>2</sub> tilted	-1.41	-0.26 -0.11	1.28	1.91/2.80
O <sub>2</sub> tilted	-1.49	-0.25 -0.11	1.27	1.92/2.82
LS50M MnO <sub>2</sub>				
O	-1.06	-0.49	n/a	1.57
O	-1.09	-0.52	n/a	1.58
O <sub>2</sub> tilted	-1.37	-0.24 -0.09	1.27	1.90/2.78
O <sub>2</sub> tilted	-1.39	-0.25 -0.09	1.28	1.90/2.78

The charges of atomic O species on the MnO<sub>2</sub> termination are much smaller than those on the AO termination, these species can rather be assigned as  $O_{ad}^-$ . In contrast to the AO termination, the O charge varies perceptibly with the average Mn oxidation state from -0.69 to -0.55  $e$  for LM (Mn<sup>3.25+</sup>) to -0.52 to -0.49  $e$  for LM (Mn<sup>3.63+</sup>), which might reflect the partially covalent Mn-O bond. A similar variation is found for the charges of adsorbed molecular species. Molecular adsorbates with O-O distance  $\leq 1.3$  Å can be assigned to superoxide ( $O_2^-$ ).

**Table A6:** Exemplary transition states for oxygen molecule dissociation on AO termination. The dissociation reaction energy  $\Delta E_{diss}$  (the variations for a given slab arise from different surface configurations, e.g. proximity of Sr), the energy of initial adsorbate state (relative to gaseous O<sub>2</sub>), absolute energy of transition state (relative to gaseous O<sub>2</sub>) and dissociation barrier (energy difference between transition state and initial adsorbed state) are summarized.

configuration	$\Delta E_{diss}$ / eV	Initial state / eV	transition state / eV	barrier / eV
LM horizontal	-2.55	-5.59	-5.21	0.38
tilted	-3.24	-4.90	-4.55	0.35
LS25M horizontal	-1.11	-4.03	-3.43	0.60
tilted	-1.98	-3.91	-3.53	0.38
tilted	-2.01	-3.45	-2.77	0.68
LS50M tilted	-0.50	-2.46	-1.16	1.30
tilted	-0.49	-2.39	-1.66	0.73
tilted	-0.44	-2.34	-1.32	1.02

**Table A7:** Critical comparison of defect concentrations, mobilities and adsorbate coverage for the two terminations. For AO, data are given for LM as well as LS50M since the values vary strongly with average Mn oxidation state. Since this variation is almost negligible for the MnO<sub>2</sub> termination, only one value is given there.

	bulk	AO termination		MnO <sub>2</sub> termination
		LM	LS50M	
difference of $E_{V_{\text{O}}^{\bullet\bullet}}$ to bulk / eV		+0.7	+0.5 Fig. 3c	-0.5 Fig. 3c
$[V_{\text{O}}^{\bullet\bullet}]$ at 1000 K, 0.2 bar O <sub>2</sub>	$\approx 10^{-9}$ <sup>i</sup>	$\approx 2 \cdot 10^{-13}$	$\approx 3 \cdot 10^{-12}$ <sup>ii</sup>	$\approx 4 \cdot 10^{-7}$ <sup>ii</sup>
$V_{\text{O}}^{\bullet\bullet}$ migration barrier / eV	0.95 <sup>[2]</sup>	1.4 <sup>iii</sup>		0.7 <sup>[2]</sup>
O <sub>ad</sub> migration barrier / eV		1.3 <sup>iv</sup>		2.0 <sup>[3]</sup>
O <sub>ad</sub> <sup>-</sup> or O <sub>ad</sub> <sup>2-</sup> coverage $2E_{\text{ad,O}} / \text{eV}$		-9	-4 Fig. 7	-2 Fig. 7
$\Delta G_{\text{ad,O}}^0 / \text{eV}$		-7.5/-7	-2.5/-2.0 <sup>v</sup>	-0.5/0.0 <sup>v</sup>
$K_{\text{ad,O}}^0$		$10^{39}/4 \cdot 10^{36}$	$10^{13}/3 \cdot 10^{10}$	400/1
coverage for 0.2 bar O <sub>2</sub>		$\approx 20$ %	$\approx 20$ % <sup>vi</sup>	$\approx 20$ % <sup>vi</sup>
O <sub>2</sub> <sup>-</sup> or O <sub>2</sub> <sup>2-</sup> coverage $E_{\text{ad,O}_2} / \text{eV}$		-5	-2.5 Fig. 7	-1.4 Fig. 7
$\Delta G_{\text{ad,O}_2}^0 / \text{eV}$		-3.5/-3.0	-1.0/-0.5 <sup>vii</sup>	+0.1/+0.5 <sup>vii</sup>
$K_{\text{ad,O}_2}^0$		$2 \cdot 10^{18}/5 \cdot 10^{15}$	$2 \cdot 10^5/400$	0.3/0.0007
coverage for 0.2 bar O <sub>2</sub>		$\approx 20$ %	$\approx 20$ % <sup>viii</sup>	$\approx 10$ % / $\approx 0.2$ % <sup>viii</sup>
dissociation barrier / eV		0.4	0.7 Tab. A5	0.6 <sup>[3]</sup>

<sup>i</sup> experimental data, derived from  $D^*$  and  $D_{V_{\text{O}}^{\bullet\bullet}}$  data in ref. <sup>[4]</sup>

<sup>ii</sup> calculated from the difference in  $E_{V_{\text{O}}^{\bullet\bullet}}$  to bulk according to

$$\text{O}_{\text{O}}^{\times} + 2\text{Mn}_{\text{Mn}}^{\times} \rightleftharpoons \text{V}_{\text{O}}^{\bullet\bullet} + 2\text{Mn}_{\text{Mn}}^{\prime} + 1/2\text{O}_2 \quad K = \frac{[\text{V}_{\text{O}}^{\bullet\bullet}][\text{Mn}_{\text{Mn}}^{\prime}]^2 \sqrt{p\text{O}_2}}{[\text{Mn}_{\text{Mn}}^{\times}]^2} = e^{-\Delta G_{V_{\text{O}}^{\bullet\bullet}}/RT}$$

$$\Rightarrow [\text{V}_{\text{O}}^{\bullet\bullet}]_{\text{surf}} = [\text{V}_{\text{O}}^{\bullet\bullet}]_{\text{bulk}} e^{(E_{V_{\text{O}}^{\bullet\bullet}}^{\text{bulk}} - E_{V_{\text{O}}^{\bullet\bullet}}^{\text{surf}})/RT}$$

assuming that the concentrations of  $[\text{Mn}_{\text{Mn}}^{\times}], [\text{Mn}_{\text{Mn}}^{\prime}]$  hardly change between surface and bulk since  $[V_{\text{O}}^{\bullet\bullet}]$  is very small. Note that in this estimate only the modified  $E_{V_{\text{O}}^{\bullet\bullet}}$  for the surface layer is considered, potential effects of modified  $\Delta S_{V_{\text{O}}^{\bullet\bullet}}^0$  in the surface layer as well as the surface dipole are ignored.

<sup>iii</sup> in contrast to the MnO<sub>2</sub> termination,  $V_{\text{O}}^{\bullet\bullet}$  migration parallel to the AO termination is possible only via the subsurface layer. Assuming that the migration barrier to/from the subsurface MnO<sub>2</sub> layer is the same as in bulk and considering a  $V_{\text{O}}^{\bullet\bullet}$  segregation energy of about 0.5 eV between subsurface and surface (Fig. 4), an overall migration energy of  $\approx 1.4$  eV is obtained

<sup>iv</sup> the energy of O<sub>ad</sub> atop La is 1.3 eV higher than O<sub>ad</sub> adsorbed in the stable "hollow" position. With a surface O<sub>ad</sub> or  $V_{\text{O}}^{\bullet\bullet}$  migration barrier of 1.3-1.4 eV on AO compared to 0.7 eV on MnO<sub>2</sub>, at 1000 K the O<sub>ad</sub>- $V_{\text{O}}^{\bullet\bullet}$  encounter rate will be lower by 3 orders of magnitude on the AO termination

<sup>v</sup>  $\Delta G_{\text{ad,O}}^0$  calculated from  $2E_{\text{ad,O}}$  assuming  $\Delta S_{\text{ad,O}}^0 = -150/-200$  J/molK for the adsorption  $\text{O}_2 + 2n\text{Mn}_{\text{Mn}}^{\prime} + 2[\dots] \rightleftharpoons 2\text{O}_{\text{ad}}^{2-} + 2n\text{Mn}_{\text{Mn}}^{\times}$  where  $[\dots]$  represents free surface adsorption sites (translational and rotational degrees of freedom of gas-phase O<sub>2</sub> molecule largely lost, cf. discussion in ref. <sup>[3]</sup>)

$$\text{vi } K_{\text{ad,O}}^0 = \frac{[\text{O}_{\text{ad}}^{n-}]^2 [\text{Mn}_{\text{Mn}}^x]^{2n}}{p\text{O}_2 [\text{Mn}_{\text{Mn}}']^{2n} [\dots]^2}. \text{ For } K_{\text{ad,O}}^0 \geq 1, \text{ this would yield very large adsorbate coverages, which}$$

cannot be realized when the adsorbed species are charged. In ref. <sup>[3]</sup> a saturation limit of about 20% coverage was estimated for this case

vii  $\Delta G_{\text{ad,O}_2}^0$  calculated from  $E_{\text{ad,O}_2}$  assuming  $\Delta S_{\text{ad,O}_2}^0 = -150/-200$  J/molK for the adsorption



$$\text{viii } K_{\text{ad,O}_2}^0 = \frac{[\text{O}_{\text{ad},2}^{n-}] [\text{Mn}_{\text{Mn}}^x]^n}{p\text{O}_2 [\text{Mn}_{\text{Mn}}']^n [\dots]}. \text{ For } K_{\text{ad,O}_2}^0 \geq 1, \text{ this would yield very large adsorbate coverages,}$$

which cannot be realized when the adsorbed species are charged. In ref. <sup>[3]</sup> a saturation limit of about 20% coverage was estimated for this case. Only for the MnO<sub>2</sub> termination, smaller coverages are obtained. For  $n = 1$  (superoxide formation), adsorption site concentration  $[\dots] \approx 1$  and the LM slab ( $\text{Mn}^{+325} \rightarrow [\text{Mn}_{\text{Mn}}'] / [\text{Mn}_{\text{Mn}}^x] = 3$ ) this yields coverages of 18% /4% for the two  $\Delta S_{\text{ad,O}_2}^0$  values; for the LS50M slab LM slab ( $\text{Mn}^{+363} \rightarrow [\text{Mn}_{\text{Mn}}'] / [\text{Mn}_{\text{Mn}}^x] = 0.6$ ) coverages of 0.04% / 0.01% are obtained.

## References

- 
- <sup>1</sup> E. A. Kotomin, R. Merkle, Y. A. Mastrikov, M. M. Kuklja and J. Maier, *ECS Transact.* 2017, 77(10), 67
  - <sup>2</sup> E. A. Kotomin, Y. A. Mastrikov, E. Heifets and J. Maier, *Phys. Chem. Chem. Phys.* 2008, 10, 4644
  - <sup>3</sup> Y. A. Mastrikov, R. Merkle, E. Heifets, E. A. Kotomin and J. Maier, *J. Phys. Chem. C* 2010, 114, 3017
  - <sup>4</sup> R. A. De Souza and J. A. Kilner, *Solid State Ionics* 1998, 106, 175